

This discussion paper is/has been under review for the journal Geoscientific Model Development (GMD). Please refer to the corresponding final paper in GMD if available.

Integrating peatlands into the coupled Canadian Land Surface Scheme (CLASS) v3.6 and the Canadian Terrestrial Ecosystem Model (CTEM) v2.0

Y. Wu¹, D. L. Verseghy¹, and J. R. Melton²

¹Climate Processes Section, Climate Research Division, Environment Canada, 4905 Dufferin Street, Toronto, ON, M3H 5T4, Canada

²Climate Processes Section, Climate Research Division, Environment Canada, at the University of Victoria, 3800 Finnerty Road, Victoria, BC, V8P 5C2, Canada

Received: 22 October 2015 – Accepted: 10 November 2015 – Published: 27 November 2015

Correspondence to: Y. Wu (yuanqiao.wu@canada.ca)

Published by Copernicus Publications on behalf of the European Geosciences Union.

GMDD

8, 10089–10143, 2015

Integrating peatlands into the coupled Canadian Land Surface Scheme

Y. Wu et al.

Title Page

Abstract

Introduction

Conclusions

References

Tables

Figures

◀

▶

◀

▶

Back

Close

Full Screen / Esc

Printer-friendly Version

Interactive Discussion



Abstract

Peatlands, which contain large carbon stocks that must be accounted for in the global carbon budget, are poorly represented in many earth system models. We integrated peatlands into the coupled Canadian Land Surface Scheme (CLASS) and the Canadian Terrestrial Ecosystem Model (CTEM), which together simulate the fluxes of water, energy and CO₂ at the land surface–atmosphere boundary in the family of Canadian Earth System Models (CanESMs). New components and algorithms were added to represent the unique features of peatlands, such as their characteristic ground floor vegetation (mosses), the slow decomposition of carbon in the water-logged soils and the interaction between the water, energy and carbon cycles. This paper presents the modifications introduced into the CLASS-CTEM modelling framework together with site-level evaluations of the model performance for simulated water, energy and carbon fluxes at eight different peatland sites. The simulated daily gross primary production and ecosystem respiration are well correlated with observations, with values of the Pearson correlation coefficient higher than 0.8 and 0.75 respectively. The simulated mean annual net ecosystem production at the eight test sites is 87 g C m⁻² yr⁻¹, which is 22 g C m⁻² yr⁻¹ higher than the observed annual mean. The general peatland model compares well with other site-level and regional-level models for peatlands, and is able to represent bogs and fens under a range of climatic and geographical conditions.

1 Introduction

Peatlands represent about 20% of the global soil carbon (C) pool and have played a critical role in regulating the global climate since the onset of the Holocene (Yu et al., 2013). Peatlands have accumulated more than 600 GtC over the Holocene and serve as a long-term C sink at a rate higher than 5 GtC per century on average (Yu et al., 2010). Over 90% of the world's peatlands are located in the Northern Hemisphere (Yu et al., 2010) in large areas such as the Hudson Bay Lowlands, the west

GMDD

8, 10089–10143, 2015

Integrating peatlands into the coupled Canadian Land Surface Scheme

Y. Wu et al.

Title Page

Abstract

Introduction

Conclusions

References

Tables

Figures



Back

Close

Full Screen / Esc

Printer-friendly Version

Interactive Discussion



CTEM directly controls the stomatal activity and the associated stomatal resistance of the PFTs and thus affects the energy and water exchanges at the surface in CLASS. Photosynthesis and leaf respiration are modelled at a time step of 30 min, whereas the rest of the terrestrial ecosystem processes are modelled at a daily time step.

To account for the eco-hydrological and biogeochemical interactions among vegetation, atmosphere and soil in peatlands, the following modifications were made to the coupled CLASS3.6-CTEM2.0 modelling framework:

1. The top soil layer was characterized as a moss layer with a higher heat and hydraulic capacity than a mineral soil layer. The moss layer buffers the exchange of energy and water at the soil surface and regulates the soil temperature and moisture (Turetsky et al., 2012).
2. Three peatland vascular PFTs (evergreen shrubs, deciduous shrubs and sedges) as well as mosses were added to the existing 9 CTEM PFTs. These peatland-specific PFTs are adapted to cold climate and inundated soil with optimized plant structure (shoot/root ratio, rooting depth), growth strategy and metabolic acclimations to light, water and temperature.
3. We considered the soil inundation stress on microbial respiration in the litter C pool. The original CTEM assumed that litter respiration was not affected by oxygen deficit as a result of flooding, since litter was always assumed to have access to air. This assumption does not hold for peatlands where high water table positions occur routinely.
4. We separated the soil C balance and heterotrophic respiration (HR) calculations for peatland and non-peatland fractions for each grid cell in the global model. Over the non-peatland fraction, we used the original CTEM approach that aggregated the HR from each PFT weighted by the fractional cover. Over the peatland fraction the soil C pool and decomposition are controlled by the water table position, following the two-compartment approach used in the MWM (St-Hilaire et al., 2010).

Integrating peatlands into the coupled Canadian Land Surface Scheme

Y. Wu et al.

Title Page

Abstract

Introduction

Conclusions

References

Tables

Figures



Back

Close

Full Screen / Esc

Printer-friendly Version

Interactive Discussion



2.1 Soil layers

The water table depth (WTD) in natural peatlands fluctuates seasonally from above the soil surface to the top of the permanently saturated soil layer, which is often referred to as the boundary between *acrotelm* and *catotelm*. The boundary is usually estimated to be 30 cm below the soil surface in wetlands (National Wetland Working Group, 1997), and has been widely used as the bottom of the first soil layer in two-layer soil decomposition models (e.g. Granberg et al., 1999; Yorova et al., 2007; Spahni et al., 2013). To capture the effect of the fluctuating water table on the transfer of water and energy within the soil, we used a multi-layer configuration rather than the standard three-layer configuration of the soil layers in CLASS. We assigned nine organic soil layers, each 10 cm thick, at the top of the soil profile and a 10th soil layer from 90 cm down to the bottom of the organic soil (Fig. 1). Moss was treated as the top first soil layer and the substrate below the 10th soil layer was considered as bedrock. Mineral soil was not included.

2.2 A moss layer as the first soil layer

The standard configuration of soil layers in CLASS consists of 3 layers with thickness of 0.10, 0.25, and 3.75 m. Organic soil in CLASS was parameterized by Letts et al. (2000) as fibric, hemic and sapric peat in the three soil layers respectively, representing fresh, moderately decomposed and highly decomposed organic matter. Tests of CLASS on peatlands revealed improved performance in the energy simulations for fens and bogs with this organic soil parameterization. However, the model overestimated energy and water fluxes at bog surfaces during dry periods due to the neglect of the moss cover (Comer et al., 2000).

To take into account the interaction amongst the moss and the soil layers and the overlying atmosphere for energy and water transfer, we added a new soil layer 0.10 m thick above the fibric organic soil to represent living and dead peatland bryophytes, such as *Sphagnum* mosses and true mosses (*Bryopsida*). The physical characteris-

GMDD

8, 10089–10143, 2015

Integrating peatlands into the coupled Canadian Land Surface Scheme

Y. Wu et al.

Title Page

Abstract

Introduction

Conclusions

References

Tables

Figures

⏪

⏩

◀

▶

Back

Close

Full Screen / Esc

Printer-friendly Version

Interactive Discussion



is completely melted.

$$G_{0,m} = \zeta \min \left(J_s, \frac{(J_c + J_e) \pm \sqrt{(J_c + J_e)^2 - 4(J_c + J_e)}}{2} \right). \quad (4)$$

The dark respiration in mosses ($R_{d,m}$) is calculated as a function of the base dark respiration rate ($R_{d,m,0}$) which has a value of $1.1 \mu\text{mol m}^{-2} \text{s}^{-1}$ (Adkinson and Humphreys, 2011) scaled by the moss moisture ($f_{m,rd}$) and soil temperature functions ($f_{T,rd}$). The MWM models the relation between water content in mosses and dark respiration with optimal water content at 5.8 g water per g dry weight, following the approach in Frohling et al. (1996). We modified the relation for water content above the optimal water content, based on a recent discovery of a weak linear positive relation between the dark respiration rate and the water content above the optimal water content during the late summer and fall (Adkinson and Humphreys, 2011)

$$R_{d,m} = R_{d,m,0} f_{m,rd} f_{T,rd} \quad (5)$$

$$f_{T,rd} = (3.22 - 0.046 \times T_{\text{moSS}})^{(T_{\text{moSS}} - 25/10)} \quad (6)$$

$$f_{m,rd} = \begin{cases} 0, & \theta_m < 0.4 \\ 0.35 \theta_m^{2/3} - 0.14, & 0.4 \leq \theta_m < 5.8 \\ 0.01 \theta_m + 0.942, & 5.8 < \theta_m \end{cases} \quad (7)$$

Photosynthetic photon flux density (PPFD) is measured by the photosynthetically active radiation (PAR), which is defined as the solar radiation between 0.4 to 0.7 μmol that can be used by plants via photosynthesis. In the coupled CLASS-CTEM system, the PAR received by the moss (PAR_m , unit $\mu\text{mol photons m}^{-2} \text{s}^{-1}$) is converted from the visible short-wave radiation reaching the ground (K_{*g} , unit: W m^{-2}) in CLASS by a factor of $4.6 \mu\text{mol m}^{-2} \text{s}^{-1}$ (McCree, 1972). K_{*g} is a function of the incoming shortwave radiation

Integrating peatlands into the coupled Canadian Land Surface Scheme

Y. Wu et al.

Title Page

Abstract

Introduction

Conclusions

References

Tables

Figures

◀

▶

◀

▶

Back

Close

Full Screen / Esc

Printer-friendly Version

Interactive Discussion



($K \downarrow$, unit: W m^{-2}), the surface albedo (α_g), and the canopy transmissivity (τ_c):

$$K_{*g} = K \downarrow \tau_c (1 - \alpha_g). \quad (8)$$

The energy uptake by the moss layer is thus a function of the total incoming short-wave radiation, the aggregated leaf area index (LAI) of the PFTs present, the snow depth, the fractional vegetation cover and the soil water content (Verseghy, 2012). In peatland C models that do not consider vegetation dynamics, the transmissivity of the vegetation canopy is usually assumed to be constant (e.g. St-Hilaire et al., 2010). Compared with such models, CLASS enables a better representation of light incident on the moss surface since it includes partitioning of direct/diffuse and visible/near-IR radiation, PFT-specific transmissivities, and time-varying LAI and fractional PFT coverages (Verseghy et al., 2012).

2.4 Peatland-specific PFTs

CLASS normally categorizes the global vegetation into 4 broad PFTs that differ in their structure and intra-annual development cycles: needleleaf trees (NDL), broadleaf trees (BDL), crops and grasses. CTEM further subdivides each PFT in CLASS into PFTs that vary in their phenology, physiology and their C assimilation rates: evergreen NDL, deciduous NDL, evergreen BDL, deciduous cold BDL, deciduous dry BDL, C3 crops, C4 crops, C3 grasses and C4 grasses. The evergreen broadleaf PFTs and C3 grasses have been parameterized primarily for tropical and temperate vegetation types that are not representative of peatland plants. Therefore, we introduced 3 new PFTs for peatlands: evergreen shrubs, deciduous shrubs and sedges. Evergreen shrubs, for example the ericaceous shrubs, are the common dominant vascular plants in bogs and poor fens while deciduous shrubs, such as the betulaceous shrubs often dominate rich fens. Both shrubs are categorized as broadleaf trees in CLASS morphologically, but their phenological and physiological characteristics are more similar to those of needleleaf trees. The shrub tundra ecosystem is situated adjacent to needleleaf forest

in the Northern Hemisphere (Kaplan et al., 2003) and they share similar responses to climate in ESMs (e.g. Bonan et al., 2002). Table 2 lists the key parameters for the peatland PFTs used in this model. (The photosynthesis and autotrophic respiration of vascular PFTs are modeled the same as the original CTEM.)

2.5 Heterotrophic respiration

Over the non-peatland fraction, heterotrophic respiration (HR) is calculated as the sum of the respiration from litter and soil carbon pools as in the original version of CTEM (Arora, 2003). The soil C pool over the non-peatland areas is assumed to be exponentially distributed with depth (Arora, 2003). In peatlands a large amount of *humic* soil is generally located in the permanently saturated zone and the bulk density increases with soil depth (Loisel and Garneau, 2010). Thus the assumption of exponentially decreasing distribution of C content with increasing soil depth is not valid in peatlands. We used a quadratic equation to calculate the distribution of soil C content over depth based on an empirically determined bulk density profile (Frolking et al., 2001).

HR over the peatland fraction of a grid cell is modelled using a two-pool approach with a flexible boundary between the pools that depends on the depth of the water table:

$$\begin{cases} R_o = C_{\text{SOM},o} k_o f_{T,o} \\ R_a = C_{\text{SOM},a} k_a f_{T,a} f_{\text{anoxic}} \end{cases} \quad (9)$$

where *o* and *a* denote the oxic and anoxic portions of the soil C pool, respectively. The respiration rate *R* (unit: $\mu\text{mol C m}^{-2} \text{s}^{-1}$) is obtained from the respiration rate constant *k* ($\mu\text{mol C kg C}^{-1} \text{s}^{-1}$), the temperature functions f_T , the soil C mass C_{SOM} (kg) and a scaling factor f_{anoxic} which is set to 0.025 (Frolking et al., 2010) representing the inhibition of microbial respiration under anoxic conditions. Q_{10} is calculated using a hyperbolic tan function of the soil temperatures (T_s) of the oxic and anoxic zones (Melton and Arora, 2015), which are in turn functions of water table depth (Eqn. 10). *k*, f_T and C_{SOM} are updated along with the water table depth (z_{wt} , unit: m, positive downward) and the peat

Integrating peatlands into the coupled Canadian Land Surface Scheme

Y. Wu et al.

Title Page

Abstract

Introduction

Conclusions

References

Tables

Figures

◀

▶

◀

▶

Back

Close

Full Screen / Esc

Printer-friendly Version

Interactive Discussion



depth (d_p , unit: m) at each CTEM time step. The equations for k and C_{SOM} are derived from Fig. 2 in Frolking et al. (2001), and parameterized differently for fens and bogs (Table 3):

$$\begin{cases} f_{T,o} = Q_{10,o}^{(\int_1^{d_{wt}} T_j - 15)/10} \\ f_{T,a} = Q_{10,a}^{(\int_1^{d_p} T_j - 15)/10} \end{cases} \quad (10)$$

$$Q_{10} = 1.44 + 0.56 \tanh[0.075(46.0 - T_s)] \quad (11)$$

$$\begin{cases} T_{s,o} = \int_1^{d_{wt}} T_j \\ T_{s,a} = \int_{d_{wt}}^{d_p} T_j \end{cases} \quad (12)$$

$$k_o = \begin{cases} 0, & z_{wt} < 0 \\ k_1(1 - e^{k_2 z_{wt}}) + k_3 z_{wt}, & 0.3 > z_{wt} \geq 0 \\ k_4 e^{k_5 z_{wt}} + k_6 z_{wt} + k_7, & z_{wt} \geq 0.3 \end{cases} \quad (13)$$

$$k_a = \begin{cases} k_4 e^{k_5 d_p} + 10k_6 d_p + k_7, & z_{wt} < 0 \\ \left| k_1 e^{k_2 z_{wt}} - k_4 e^{k_5 d_p} - k_3 z_{wt} + k_8 \right|, & 0.3 > z_{wt} \geq 0 \\ k_4 (e^{k_5 d_p} - e^{k_5 z_{wt}}) + k_6 (d_p - z_{wt}), & z_{wt} \geq 0.3 \end{cases} \quad (14)$$

$$C_{SOM,o} = 0.487 \times (k_9 z_{wt}^2 + k_{10} z_{wt}) \quad (15)$$

$$C_{SOM,a} = C_{SOM} - C_{SOM,o}, \quad (16)$$

where 0.487 is a parameter that converts from soil mass to soil C content. As only organic soil is considered in peatlands, the peat soil C is updated from the humification (C_{hum} kg C m⁻² day⁻¹) and soil respiration from the oxic (R_o in kg C m⁻² day⁻¹) and

anoxic (R_a in $\text{kg C m}^{-2} \text{ day}^{-1}$) components during the time step:

$$\frac{dC_{\text{SOM}}}{dt} = C_{\text{hum}} - R_o - R_a. \quad (17)$$

At the end of each time step, the peat depth (i.e. the depth of the organic soil) d_p is updated from the updated peat C mass (C_{SOM} in kg) by solving the quadratic equation:

$$d_p = \frac{-k_{10} + \sqrt{k_{10}^2 + \frac{4 \text{ kg } C_{\text{SOM}}}{0.487}}}{2 \text{ kg}}. \quad (18)$$

The water table depth z_{wt} is deduced by searching for a soil layer below which the soil is saturated and above which the soil moisture is at or below the retention capacity with respect to gravitational drainage. Within this soil layer j , z_{wt} is calculated as:

$$z_{\text{wt}} = z_{b,j} - \Delta z \left[\frac{\theta_{l,j} + \theta_{i,j} - \theta_{\text{ret},j}}{\theta_{p,j} - \theta_{\text{ret},j}} \right], \quad (19)$$

where Δz is the thickness of soil layer (unit: m), θ_l and θ_i are the liquid and frozen water contents (unit, $\text{m}^3 \text{ m}^{-3}$), θ_{ret} and θ_p are the water retention capacity and the porosity, and z_b (unit: m) is the bottom depth of the soil layer.

3 Evaluation methods and data

3.1 Site locations

The model was applied at eight peatland sites to assess its performance in simulating the water, energy and C fluxes. Data were obtained from the FLUXNET database (<http://fluxnet.ornl.gov/>). The peatlands selected consist of four bogs and four fens (Fig. 2). The bogs are the Auchecorth Moss (UK-Amo), 18 km south of Edinburgh,

3.4 Evaluation methods

The model was evaluated against observation-based sensible and latent heat fluxes at the soil surface, soil water content, water table and snow depth, soil temperature at various depths and the daily, monthly and annual C fluxes (GPP, ER, NEP). The root mean square error (RMSE) and linear regression coefficient (r^2) were primarily used for evaluation. Statistical analyses were conducted using the free software package R version 3.1.1 (R Core Team, 2014).

Since the ultimate goal is to apply the model globally in an ESM, further experiments were done to investigate the importance of modelling fens and bogs separately. In the version of the model described above, bogs and fens are distinguished primarily through the parameterization of the control of water table depth on soil decomposition (Table 3). Also, the depth of the living moss (d_m) is set to 4.0 cm for bogs and 3.0 cm for fens. In a first test, the parameters for soil decomposition (Table 3) for bogs were used for the fen sites and those for the fens were used for the bog sites. In a second test, the living moss layer was set to a set to a single fixed value of 3.5 cm for both bogs and fens. The resulting differences in the surface fluxes and the soil temperatures were then evaluated.

4 Results and discussion

4.1 Water budget terms

Figure 3 illustrates the simulated daily WTD compared with observations at the six sites where WTD was observed. The model successfully simulated the seasonal dynamics and the zone of fluctuation of the water table in the first two bogs, except for the extremely deep water table observed in RU-Fyo in 2010. Although ponded water is simulated in the model, the simulated WTD did not include the depth of pond above the soil surface, which appears in the observations as a negative value, for example

Integrating peatlands into the coupled Canadian Land Surface Scheme

Y. Wu et al.

Title Page

Abstract

Introduction

Conclusions

References

Tables

Figures



Back

Close

Full Screen / Esc

Printer-friendly Version

Interactive Discussion



Integrating peatlands into the coupled Canadian Land Surface Scheme

Y. Wu et al.

Title Page

Abstract

Introduction

Conclusions

References

Tables

Figures



Back

Close

Full Screen / Esc

Printer-friendly Version

Interactive Discussion

into CLASS by Comer et al. (2000), RMSEs ranged from 16.9 to 47.7 W m^{-2} (QH) and 23.1 to 65.6 W m^{-2} (QE) for fens and from 67.4 to 182.5 W m^{-2} (QH) and 78.1 to 153.8 W m^{-2} (QE) for bogs. Our new model shows a consistent improvement in the energy flux simulations, especially for bogs, where the surface moss cover plays an essential role in regulating the thermal and hydraulic conductivities (Turetsky et al., 2012).

The mean r^2 coefficient between the simulated and observed QH was 0.47 and the highest r^2 was 0.89 for the AB-Fen site. The poorest agreement in QH occurred in the FI-Kaa fen and the UK-Amo bog. The error in FI-Kaa peaked in the winters of 2002 and 2007 when the snow depth exceeded 0.8 m (not shown). Turbulent fluxes over deep, cold snow packs are notoriously difficult to model accurately (Bazile et al., 2013). In the case of QE, the mean r^2 for the 8 sites is 0.52, and rises to 0.60 if the outlier UK-Amo is disregarded. The large bias of QH and QE at UK-Amo is thought to be partially attributable to instrumental errors, given the scattered data cloud of the observed QE in 2006 (not shown).

The simulated soil temperature at 5 cm depth across the eight sites agreed well with the observations, with r^2 values between 0.77 and 0.98. The comparatively low value found for UK-Amo is perhaps linked to the errors in QE noted above. The RMSE ranged from 1.7 to 4.7 $^{\circ}\text{C}$ with a mean of 3.1 $^{\circ}\text{C}$. This is larger than the RMSE range of 0.7 to 2.3 $^{\circ}\text{C}$ found for LPJ-WHy v1.2 by Wania et al. (2009a), yet is encouraging considering that the simulation periods for our sites ranged from 2 to 9 years compared to the 1 year simulation with LPJ-WHy, and that we included eight sites in our evaluation compared with two peatland sites for LPJ-WHy. Our model was able to capture the seasonal variation in soil temperature at different depths down to the bedrock. Figure 6 compares the modeled soil temperatures against the observations at 5, 40, 80, and 250 cm depths for the Mer Bleue bog, where good-quality data are available for soil T at various depths.

4.3 Carbon fluxes

Examination of the modelled GPP, ER and NEP demonstrates that the model is capable of capturing seasonal dynamics and climate-driven events consistently in various types of peatlands (Figs. 7–9). For example, the RU-Fyo bog experienced a period of low GPP due to an abrupt decrease of air temperature in the early fall of 2010, which was well reproduced by the model. The RMSE (Table 6) was around $0.60 \text{ gC m}^{-2} \text{ day}^{-1}$ for GPP and ER for the three sites in Scandinavia and Canada (FI-Kaa, MB-Bog, and SE-Faj) that have high-quality observed data and are not undergoing vegetation shifts. Larger biases of GPP and ER occurred in the blanket bog (UK-Amo) and the Russian ombrotrophic bog (RU-Fyo), the peat depths of which were very deep and relatively shallow respectively – up to 10 m in UK-Amo and 1 m in RU-Fyo (Table 4). Variations in the historical climate have led to variations in the peat accumulation rates over the Holocene and the vertical stratification of the peat and hence the decomposition rates and decomposability of the peat, which becomes important for deeper, older peat deposits. The Russian bog may be an outlier because warm climate conditions persisted until about 5000 BP in Northern Siberia and about 1000 years later in most other areas (Yu et al., 2009). The starting and ending periods of photosynthesis in the spring and fall were accurately simulated except for the coldest peatland, FI-Lom, where the length of the growing season was slightly overestimated. Short periods of overestimation of soil temperature at 5 cm existed during that period, by up to 5°C , which may have caused the errors in GPP; Moore et al. (2012) noted a high correlation between soil temperature and the initiation of photosynthesis in the spring.

NEP is calculated by subtracting ER from GPP, therefore the bias in the NEP simulations compared with observations accumulates from the biases in GPP and ER. The RMSE of the daily NEP simulations ranges from 0.486 to $1.633 \text{ gC m}^{-2} \text{ day}^{-1}$. The lowest biases were for the SE-Faj bog and the two poor fens (SE-Deg and FI-Kaa) that had little vegetation cover, with the maximum LAI below $1.0 \text{ m}^2 \text{ m}^{-2}$. Values of r^2 greater than 0.3 were observed at six sites. At the two others, SE-Faj and UK-Amo, the

GMDD

8, 10089–10143, 2015

Integrating peatlands into the coupled Canadian Land Surface Scheme

Y. Wu et al.

Title Page

Abstract

Introduction

Conclusions

References

Tables

Figures



Back

Close

Full Screen / Esc

Printer-friendly Version

Interactive Discussion



observed NEP varied widely, ranging from -1.8 to $2.2 \text{ gC m}^{-2} \text{ day}^{-1}$ and from -3.9 to $4.8 \text{ gC m}^{-2} \text{ day}^{-1}$ respectively. Model errors for the extreme values at these two sites may have contributed to their low r^2 values. NEP was overestimated at the beginning and the end of the growing season for FI-Lom due to the overestimation of GPP for that period as discussed above. These results may be compared to an evaluation of the MWM using the SE-Deg dataset that was conducted by Wu et al. (2013). For daily NEP they obtained an RMSE of 0.49, similar to ours, but a higher r^2 of 0.52. It should be noted that the MWM was driven by observed WTD and soil temperature, while in our simulations these were allowed to evolve freely, so our reasonable result is encouraging.

The simulated accumulated monthly NEP from March to November agreed well with the observations in the four bogs and four fens. The outliers for bogs were the overestimations in MB-Bog in October and November due to the underestimation of GPP (Fig. 7). The NEP in RU-Fyo in one August was underestimated owing to the underestimated GPP, which in turn was a result of the underestimated LAI and rooting depth temperature in the summer. Figure 10, showing plots of NEP averaged for each month of the year at each site, demonstrates on the whole larger scatter for the bogs than the fens, with the scatter increasing through the summer and fall. The overall value of r^2 was 0.59 for bogs and 0.58 for fens; both values are higher than or similar to those obtained in evaluations of other peatland C models. For example, the r^2 value of the monthly NEP for LPJ-WHy was reported to be 0.35 for four peatlands, with three of the sites overlapping those used in this study: SE-Deg, FI-Kaa and MB-Bog (Wania et al., 2009b). The Finland peatland model simulated the NEP in FI-Kaa with r^2 of 0.80 for the same time period tested for our model (Gong et al., 2013), but only the one site was used in the evaluation.

Integrating peatlands into the coupled Canadian Land Surface Scheme

Y. Wu et al.

[Title Page](#)[Abstract](#)[Introduction](#)[Conclusions](#)[References](#)[Tables](#)[Figures](#)[⏪](#)[⏩](#)[◀](#)[▶](#)[Back](#)[Close](#)[Full Screen / Esc](#)[Printer-friendly Version](#)[Interactive Discussion](#)

4.4 Annual carbon budget

The simulated mean annual NEP values with their standard deviations generally fall within the range of the standard deviations of the observations (Fig. 11), between $9 \text{ gCm}^{-2} \text{ yr}^{-1}$ in the rich fen (FI-Lom) and $73 \text{ gCm}^{-2} \text{ yr}^{-1}$ in the productive bog (RU-Fyo) (Table 7). The only site with large bias in annual NEP was AB-Fen. Observation-based estimations of NEP in this fen were extremely high, totalling 176 gC from May to October, in comparison with other sites (Syed et al., 2006). This treed fen had a high peat density and LAI and large variation in the WTD, which, accompanied by high spring temperatures, resulted in high ecosystem photosynthesis capacity and production (Adkinson et al., 2010). Considering nutrient factors and the site-specific peat density could potentially capture the large NEP at this site. The observed annual NEP for the eight sites varied greatly overall, between -17 and $187 \text{ gCm}^{-2} \text{ yr}^{-1}$, while the simulated NEP showed slightly less variation, ranging from 13 to $157 \text{ gCm}^{-2} \text{ yr}^{-1}$. The simulated mean annual NEP across the sites was $87 \text{ gCm}^{-2} \text{ yr}^{-1}$ and was $22 \text{ gCm}^{-2} \text{ yr}^{-1}$ higher than the mean observed NEP. In contrast the LPJ-WHY model simulated most of the annual NEP between -5 to $0 \text{ gCm}^{-2} \text{ yr}^{-1}$, lower than their observed median of $40 \text{ gCm}^{-2} \text{ yr}^{-1}$ (Wania et al., 2009b). As noted above, variations in the depth and age of the peat at the eight sites reflected fluctuations in past climate, leading to site-specific soil properties that were not always captured by the standardized values used in the model. Peatlands in different geographical locations also reflected the effects of local conditions: for example, the blanket bog UK-Amo in a maritime climate accumulated $101 \text{ gCm}^{-2} \text{ yr}^{-1}$ in 2007 (Dinsmore et al., 2010) while the dry MB-Bog was estimated to be a source of $13.8 \text{ gCm}^{-2} \text{ yr}^{-1}$ (Roulet et al., 2007). The modeled NEP bias tended towards underestimation for the treed fen (AB-fen) and the productive ombrotrophic bog (MB-Bog), and towards overestimation for the remaining sites (Fig. 11).

The model errors in GPP were smaller than the standard deviation of the observations, except for the atypical sites (AB-Fen, RU-Fyo) and the sites that had only a few years of data (FI-Lom, SE-Faj) (Table 7). The bias of the simulated ER did not exceed

GMDD

8, 10089–10143, 2015

Integrating peatlands into the coupled Canadian Land Surface Scheme

Y. Wu et al.

Title Page

Abstract

Introduction

Conclusions

References

Tables

Figures



Back

Close

Full Screen / Esc

Printer-friendly Version

Interactive Discussion



Integrating peatlands into the coupled Canadian Land Surface Scheme

Y. Wu et al.

Title Page

Abstract

Introduction

Conclusions

References

Tables

Figures

◀

▶

◀

▶

Back

Close

Full Screen / Esc

Printer-friendly Version

Interactive Discussion



the error bars except for in the RU-Fyo bog, for which a thin peat depth of 1 m was used to initialize the simulation (Table 4). The simulated WTD was consistently shallower in the summer than the observations (Fig. 3), which slowed down the soil respiration in the model and contributed to the discrepancies in ER. The observed WTD showed an abrupt decrease in the summer of 2010 without pulses of large ER being observed during that period (Fig. 8), indicating uncertainties in the WTD observations. Another reason for the errors in ER was the underestimation in soil T . For example, the simulated soil T at 5 cm depth was higher in the summers with RMSE of 4.6 °C in RU-Fyo (Table 5). The site is particularly shallow and homogeneous, thus the standardized living moss layer of 4 cm for bogs was probably too large, leading to an overestimation of the thermal insulation effect from the moss layers and hence less seasonal variation in soil temperature and ER.

An overview of the model's performance is illustrated via a Taylor diagram (Fig. 12). This demonstrates the model's skill in simulating the hydrological and thermal dynamics and C fluxes in different types of peatlands across a variety of climatic and geographical settings. The outliers are the vegetated treed fen (AB-Fen), the maritime blanket bog UK-Amo and the extremely shallow peatland RU-Fyo. The model simulations consistently agreed quite well with the observations except at these sites for some evaluated parameters. The Pearson r was above 0.90 for the soil temperature at 5 cm and above 0.50 and 0.60 for the sensible and latent heat fluxes, except for those at UK-Amo. The soil water content at the surface soil layer, corresponding to the available measurements of soil temperature at 5 cm depth, was about 0.6 with RMSE between 0.20 and 0.28 m³ m⁻³. The modeled daily GPP and ER were highly correlated with the observations, with Pearson r values between 0.80 and 0.95 for GPP, and between 0.75 and 0.96 for ER. The simulated daily NEP accumulated the errors in GPP and ER and was somewhat less well correlated with the observations, with Pearson r values between 0.4 and 0.72.

4.5 The necessity of distinguishing fens and bogs

The original version of our peatland model (referred to as “*CONTROL*” hereafter) as described above distinguishes bogs and fens through the controls of water table depth on soil decomposition and the depth of the living moss. The parameters for the water table depth regulation of soil decomposition were derived from the empirical relations in the MWM (Eqs. 13 and 14). Our first test, “*K-SWAP*”, involved swapping the values of the decomposition parameters (Table 3) between the bog and fen sites. As shown in Fig. 13, the differences between the test and control runs are minimal. The relative differences in the simulated values of the fluxes and temperatures between *K-SWAP* and *CONTROL* ranged from -1.6 to $+5.1$ % for RMSE and from -23 to $+6$ % for r^2 . The relative differences in RMSE and r^2 for GPP, QH, QE and T_{s5} were smaller than ± 1 %. The largest differences in r^2 between *K-SWAP* and *CONTROL* were for NEP at SE-Faj and UK-Amo, which had significantly lower r^2 values than the other sites. The results of *K-SWAP* indicate that parameterizing fens and bogs differently for the regulation of water table depth on soil decomposition makes little difference in the simulation.

The second test, “*D-MOSS*”, retained the settings in *K-SWAP* and changed additionally the depth of the living moss in both bogs and fens to 3.5 cm. The RMSE and r^2 of *D-MOSS* show site-specific differences compared to *CONTROL* (Fig. 13). The relative differences between *D-MOSS* and *CONTROL* in RMSE and r^2 were in the range of -5 to $+7$ % and -15 to $+13$ %, respectively. The mean differences for all sites and all evaluated variables were less than 5 % for both RMSE and r^2 . For GPP, ER and the soil temperature at 5 cm depth, the r^2 in *D-MOSS* was similar to that of *CONTROL*. For QE, the r^2 in *D-MOSS* was higher than the control for all the fens and one unusual bog (UK-Amo), but not for the other three bogs. Compared to *CONTROL*, the r^2 of NEP was higher in *D-MOSS* for five sites by up to 7 % and less than 2 % lower in the other sites, except for UK-Amo where r^2 was also low in *CONTROL*. This test indicates that the depth of living moss is important for modeling energy exchange and

GMDD

8, 10089–10143, 2015

Integrating peatlands into the coupled Canadian Land Surface Scheme

Y. Wu et al.

Title Page

Abstract

Introduction

Conclusions

References

Tables

Figures

◀

▶

◀

▶

Back

Close

Full Screen / Esc

Printer-friendly Version

Interactive Discussion



References

- Ångström, A.: A study of the radiation of the atmosphere, *Smithson, Misc. Collect.*, 65, 1–159, 1918.
- Adkinson, A. C. and Humphreys, E. R.: The response of carbon dioxide exchange to manipulations of Sphagnum water content in an ombrotrophic bog, *Ecohydrology*, 4, 733–743, doi:10.1002/eco.171, 2011.
- Adkinson, A. C., Syed, K. H., and Flanagan, L. B.: Contrasting responses of growing season ecosystem CO₂ exchange to variation in temperature and water table depth in two peatlands in northern Alberta, Canada. *J. Geophys. Res., Biogeosciences (2005–2012)*, 116, 2011.
- Arora, V. K.: Simulating energy and carbon fluxes over winter wheat using coupled land surface and terrestrial ecosystem models, *Agr. Forest Meteorol.*, 118, 21–47, 2003.
- Arora, V. K. and Boer, G. J.: A parameterization of leaf phenology for the terrestrial ecosystem component of climate models, *Glob. Change Biol.*, 11, 39–59, doi:10.1111/j.1365-2486.2004.00890.x, 2005.
- Aurela, M., Tuovinen, J.-P., and Laurila, T.: Carbon dioxide exchange in a subarctic peatland ecosystem in northern Europe measured by the eddy covariance technique, *J. Geophys. Res.-Atmos.*, 103, 11289–11301, 1998.
- Aurela, M., Lohila, A., Tuovinen, J.-P., Hatakka, J., Riutta, T., and Laurila, T.: Carbon dioxide exchange on a northern boreal fen, *Boreal Environ. Res.*, 14, 699–710, 2009.
- Bazile, E., Traullé, O., Barral, H., Vihma, T., Holtslag, A. A. M., and Svensson, G.: GABLS4: an intercomparison case for 1D models to study the stable boundary layer at Dome-C on the Antarctic plateau, *EMS Annual Meeting Abstracts, Vol. 10, EMS2013-578*, 2013.
- Ballantyne, A. P., Alden, C. B., Miller, J. B., Tans, P. P., and White, J. W. C.: Increase in observed net carbon dioxide uptake by land and oceans during the past 50 years, *Nature*, 488, 70–72, 2012.
- Bellisario, L. M., Boudreau, L. D., Versegny, D. L., Rouse, W. R., and Blanken, P. D.: Comparing the performance of the Canadian land surface scheme (CLASS) for two subarctic terrain types, *Atmos. Ocean*, 38, 181–204, 2000.
- Beringer, J., Lynch, A. H., Chapin III, F. S., Mack, M., and Bonan, G. B.: The representation of arctic soils in the land surface model: the importance of mosses, *J. Climate*, 14, 3324–3335, 2001.

Integrating peatlands into the coupled Canadian Land Surface Scheme

Y. Wu et al.

Title Page

Abstract

Introduction

Conclusions

References

Tables

Figures

◀

▶

◀

▶

Back

Close

Full Screen / Esc

Printer-friendly Version

Interactive Discussion



Integrating peatlands into the coupled Canadian Land Surface Scheme

Y. Wu et al.

Title Page

Abstract

Introduction

Conclusions

References

Tables

Figures

◀

▶

◀

▶

Back

Close

Full Screen / Esc

Printer-friendly Version

Interactive Discussion



- Bohn, T. J., Melton, J. R., Ito, A., Kleinen, T., Spahni, R., Stocker, B. D., Zhang, B., Zhu, X., Schroeder, R., Glagolev, M. V., Maksyutov, S., Brovkin, V., Chen, G., Denisov, S. N., Eliseev, A. V., Gallego-Sala, A., McDonald, K. C., Rawlins, M. A., Riley, W. J., Subin, Z. M., Tian, H., Zhuang, Q., and Kaplan, J. O.: WETCHIMP-WSL: intercomparison of wetland methane emissions models over West Siberia, *Biogeosciences Discuss.*, 12, 1907–1973, doi:10.5194/bgd-12-1907-2015, 2015.
- Bonan, G. B., Levis, S., Kergoat, L., and Oleson, K. W.: Landscapes as patches of plant functional types: an integrating concept for climate and ecosystem models, *Global Biogeochem. Cy.*, 16, doi:10.1029/2000GB001360, 2002.
- Bond-Lamberty, B., Gower, S. T., and Ahl, D. E.: Improved simulation of poorly drained forests using Biome-BGC, *Tree Physiol.*, 27, 703–715, 2007.
- Brovkin, V., Boysen, L., Arora, V. K., Boisier, J. P., Cadule, P., Chini, L., Claussen, M., Friedlingstein, P., Gayler, V., van den Hurk, B. J. J. M., Hurtt, G. C., Jones, C. D., Kato, E., de Noblet-Ducoudré, N., Pacifico, F., Pongratz, J., and Weiss, M.: Effect of anthropogenic land-use and land-cover changes on climate and land carbon storage in CMIP5 projections for the twenty-first century, *J. Climate*, 26, 6859–6881, doi:10.1175/JCLI-D-12-00623.1, 2013.
- Bubier, J. L., Moore, T. R., and Crosby, G.: Fine-scale vegetation distribution in a cool temperate peatland, *Botany*, 84, 910–923, 2006.
- Camill, P. and Clark, J. S.: Long-term perspectives on lagged ecosystem responses to climate change: permafrost in boreal peatlands and the grassland/woodland boundary, *Ecosystems*, 3, 534–544, 2000.
- Canada Committee on Ecological (Biophysical) Land Classification, National Wetlands Working Group: The Canadian wetland classification system, edited by: Warner, B. G., and Rubec, C. D. A., Wetlands Research Branch, University of Waterloo, Waterloo, Canada, 1997.
- Christensen, J. H., Kumar, K. K., Aldrian, E., An, S.-I., Cavalcanti, I. F. A., de Castro, M., Dong, W., Goswami, P., Hall, A., Kanyanga, J. K., Kitoh, A., Kossin, J., Lau, N.-C., Renwick, J., Stephenson, D. B., Xiem, S.-P., and Zhou, T.: Climate Phenomena and their Relevance for Future Regional Climate Change, in: *Climate Change 2013: the Physical Science Basis*, Contribution of Working Group I to the Fifth Assessment Report of the Intergovernmental Panel on Climate Change, edited by: Stocker, T. F., Qin, D., Plattner, G.-K., Tignor, M., Allen, S. K., Boschung, J., Nauels, A., Xia, Y., Bex, V., and Midgley, P. M., Cambridge University Press, Cambridge, UK and New York, NY, USA, 2013.

Integrating peatlands into the coupled Canadian Land Surface Scheme

Y. Wu et al.

Title Page

Abstract

Introduction

Conclusions

References

Tables

Figures

⏪

⏩

◀

▶

Back

Close

Full Screen / Esc

Printer-friendly Version

Interactive Discussion



Comer, N. T., Lafleur, P. M., Roulet, N. T., Letts, M. G., Skarupa, M., and Verseghy, D.: A test of the Canadian Land Surface Scheme (CLASS) for a variety of wetland types, *Atmos. Ocean*, 38, 161–179, 2000.

Crawford, T. M. and Duchon, C. E.: An improved parameterization for estimating effective atmospheric emissivity for use in calculating daytime downwelling longwave radiation, *J. Appl. Meteorol.*, 38, 474–480, 1999.

Dorrepaal, E., Toet, S., van Logtestijn, R. S. P., Swart, E., van de Weg, M. J., Callaghan, T. V., and Aerts, R.: Carbon respiration from subsurface peat accelerated by climate warming in the subarctic, *Nature*, 460, 616–619, 2009.

Dimitrov, D. D., Grant, R. F., Lafleur, P. M., and Humphreys, E. R.: Modeling the effects of hydrology on ecosystem respiration at Mer Bleue bog, *J. Geophys. Res.*, 115, G04043, doi:10.1029/2010JG001312, 2010.

Dinsmore, K. J., Billett, M. F., Skiba, U. M., Rees, R. M., Drewer, J., and Helfter, C.: Role of the aquatic pathway in the carbon and greenhouse gas budgets of a peatland catchment, *Glob. Change Biol.*, 16, 2750–2762, 2010.

Drewer, J., Lohila, A., Aurela, M., Laurila, T., Minkinen, K., Penttilä T., Dinsmore, K. J., McKenzie, R. M., Helfter, C., Flechard, C., Sutton, M. A., and Skiba, U. M.: Comparison of greenhouse gas fluxes and nitrogen budgets from an ombrotrophic bog in Scotland and a minerotrophic sedge fen in Finland, *Eur. J. Soil Sci.*, 61, 640–650, 2010.

Ekici, A., Beer, C., Hagemann, S., Boike, J., Langer, M., and Hauck, C.: Simulating high-latitude permafrost regions by the JSBACH terrestrial ecosystem model, *Geosci. Model Dev.*, 7, 631–647, doi:10.5194/gmd-7-631-2014, 2014.

Flanagan, L. B. and Syed, K. H.: Stimulation of both photosynthesis and respiration in response to warmer and drier conditions in a boreal peatland ecosystem, *Glob. Change Biol.*, 17, 2271–2287, 2011.

Frolking, S., Goulden, M. L., Wofsy, S. C., Fan, S.-M., Sutton, D. J., Munger, J. W., Bazzaz, A. M., Daube, B. C., Crill, P. M., Aber, J. D., Band, L. E., Wang, X., Savage, K., Moore, T., and Harriss, R. C.: Modelling temporal variability in the carbon balance of a spruce/moss boreal forest, *Glob. Change Biol.*, 2, 343–366, 1996.

Frolking, S., Roulet, N. T., Tuittila, E., Bubier, J. L., Quillet, A., Talbot, J., and Richard, P. J. H.: A new model of Holocene peatland net primary production, decomposition, water balance, and peat accumulation. *Earth Syst. Dynam.*, 1, 1–21, 2010.

Integrating peatlands into the coupled Canadian Land Surface Scheme

Y. Wu et al.

Title Page

Abstract

Introduction

Conclusions

References

Tables

Figures

◀

▶

◀

▶

Back

Close

Full Screen / Esc

Printer-friendly Version

Interactive Discussion



- Givnish, T. J.: Adaptive significance of evergreen vs. deciduous leaves: solving the triple paradox, *Silva Fenn.*, 36, 703–743, 2002.
- Gong, J., Kellomäki, S., Wang, K., Zhang, C., Shurpali, N., and Martikainen, P. J.: Modeling CO₂ and CH₄ flux changes in pristine peatlands of Finland under changing climate conditions, *Ecol. Model.*, 263, 64–80, 2013.
- Granberg, G., Grip, H., Lövvenius, M. O., Sundh, I., Svensson, B. H., and Nilsson, M.: A simple model for simulation of water content, soil frost, and soil temperatures in boreal mixed mires, *Water Resour. Res.*, 35, 3771–3782, 1999.
- Hayward, P. M. and Clymo, R. S.: Profiles of water content and pore size in Sphagnum and peat, and their relation to peat bog ecology, *P. Roy. Soc. Lond. B. Bio.*, 215, 299–325, 1982.
- Ise, T., Dunn, A. L., Wofsy, S. C., and Moorcroft, P. R.: High sensitivity of peat decomposition to climate change through water-table feedback, *Nat. Geosci.*, 1, 763–766, 2008.
- Kaplan, J. O., Bigelow, N. H., Prentice, I. C., Harrison, S. P., Bartlein, P. J., Christensen, T. R., Cramer, W., Matveyeva, N. V., McGuire, A. D., Murray, D. F., Razzhivin, V. Y., Smith, B., Walker, D. A., Anderson, P. M., Andreev, A. A., Brubaker, L. B., Edwards, M. E., and Lozhkin, A. V.: Climate change and Arctic ecosystems: 2. modeling, paleodata-model comparisons, and future projections, *J. Geophys. Res.-Atmos.*, 108, doi:10.1029/2002JD002559, 2003.
- Kleinen, T., Brovkin, V., and Schuldt, R. J.: A dynamic model of wetland extent and peat accumulation: results for the Holocene, *Biogeosciences*, 9, 235–248, 2012, <http://www.biogeosciences.net/9/235/2012/>.
- Kottek, M., Grieser, J., Beck, C., Rudolf, B., and Rubel, F.: World Map of the Köppen–Geiger climate classification updated, *Meteorol. Z.*, 15, 259–263, doi:10.1127/0941-2948/2006/0130, 2006.
- Lafleur, P. M., Hember, R. A., Admiral, S. W., and Roulet, N. T.: Annual and seasonal variability in evapotranspiration and water table at a shrub-covered bog in southern Ontario, Canada, *Hydrol. Process.*, 19, 3533–3550, 2005.
- Laine, A. M., Bubier, J., Riutta, T., Nilsson, M. B., Moore, T. R., Vasander, H., and Tuittila, E.-S.: Abundance and composition of plant biomass as potential controls for mire net ecosystem CO₂ exchange, *Botany*, 90, 63–74, 2011.
- Lee, T. J. and Pielke, R. A.: Estimating the soil surface specific humidity, *J. Appl. Meteorol.*, 31, 480–484, 1992.

Integrating peatlands into the coupled Canadian Land Surface Scheme

Y. Wu et al.

Title Page

Abstract

Introduction

Conclusions

References

Tables

Figures

⏪

⏩

◀

▶

Back

Close

Full Screen / Esc

Printer-friendly Version

Interactive Discussion



Leith, F. I., Garnett, M. H., Dinsmore, K. J., Billett, M. F., and Heal, K. V.: Source and age of dissolved and gaseous carbon in a peatland–riparian–stream continuum: a dual isotope (^{14}C and $\delta^{13}\text{C}$) analysis, *Biogeochemistry*, 119, 415–433, 2014.

Letts, M. G., Roulet, N. T., Comer, N. T., Skarupa, M. R., and Verseghy, D. L. : Parametrization of Peatland Hydraulic Properties for the Canadian Land Surface Scheme, *Atmosphere-Ocean (Canadian Meteorological & Oceanographic Society)*, 38, 141–160, doi:10.1080/07055900.2000.9649643, 2000.

Lloyd, C. R., Harding, R. J., Friborg, T., and Aurela, M.: Surface fluxes of heat and water vapour from sites in the European Arctic, *Theor. Appl. Climatol.*, 70, 19–33, 2001.

Loisel, J. and Garneau, M.: Late Holocene paleoecohydrology and carbon accumulation estimates from two boreal peat bogs in eastern Canada: potential and limits of multi-proxy archives, *Palaeogeogr. Palaeoclimatol.*, 291, 493–533, 2010.

Lund, M., Lindroth, A., Christensen, T. R., and Ström, L.: Annual CO_2 balance of a temperate bog, *Tellus B*, 59, 804–811, 2007.

Maanavilja, L., Riutta, T., Aurela, M., Pulkkinen, M., Laurila, T., and Tuittila, E.-S.: Spatial variation in CO_2 exchange at a northern aapa mire, *Biogeochemistry*, 104, 325–345, 2011.

McCarter, C. P. R. and Price, J. S.: Ecohydrology of Sphagnum moss hummocks: mechanisms of capitula water supply and simulated effects of evaporation, *Ecohydrology*, 7, 33–44, doi:10.1002/eco.1313, 2012.

McCree, K. J.: Test of current definitions of photosynthetically active radiation against leaf photosynthesis data, *Agr. Meteorol.*, 10, 443–453, 1972.

Melton, J. R. and Arora, V. K.: Sub-grid scale representation of vegetation in global land surface schemes: implications for estimation of the terrestrial carbon sink, *Biogeosciences*, 11, 1021–1036, 2014,

<http://www.biogeosciences.net/11/1021/2014/>.

Melton, J. R. and Arora, V. K.: Competition between plant functional types in the Canadian Terrestrial Ecosystem Model (CTEM) v. 2.0, *Geosci. Model Dev. Discuss.*, 8, 4851–4948, doi:10.5194/gmdd-8-4851-2015, 2015.

Moore, T. R., Bubier, J. L., Frolking, S. E., Lafleur, P. M., and Roulet, N. T.: Plant biomass and production and CO_2 exchange in an ombrotrophic bog, *J. Ecol.*, 90, 25–36, 2002.

Moore, T. R., Lafleur, P. M., Poon, D. M., Heumann, B. W., Seaquist, J. W., and Roulet, N. T.: Spring photosynthesis in a cool temperate bog, *Glob. Change Biol.*, 12, 2323–2335, 2006.

Integrating peatlands into the coupled Canadian Land Surface Scheme

Y. Wu et al.

Title Page

Abstract

Introduction

Conclusions

References

Tables

Figures



Back

Close

Full Screen / Esc

Printer-friendly Version

Interactive Discussion



Munir, T. M., Xu, B., Perkins, M., and Strack, M.: Responses of carbon dioxide flux and plant biomass to water table drawdown in a treed peatland in northern Alberta: a climate change perspective, *Biogeosciences*, 11, 807–820, doi:10.5194/bg-11-807-2014, 2014.

Murphy, M. T., McKinley, A., and Moore, T. R.: Variations in above-and below-ground vascular plant biomass and water table on a temperate ombrotrophic peatland, *Botany*, 87, 845–853, 2009.

O'Donnell, J. A., Romanovsky, V. E., Harden, J. W., and McGuire, A. D.: The effect of moisture content on the thermal conductivity of moss and organic soil horizons from black spruce ecosystems in interior Alaska, *Soil Sci.*, 174, 646–651, 2009.

Olivas, P. C., Oberbauer, S. F., Tweedie, C., Oechel, W. C., Lin, D., and Kuchy, A.: Effects of fine-scale topography on CO₂ flux components of Alaskan Coastal Plain Tundra: response to contrasting growing seasons, *Arct. Antarct. Alp. Res.*, 43, 256–266, 2011.

Peichl, M., Öquist, M., Löfvenius, M. O., Ilstedt, U., Sagerfors, J., Grelle, A., Lindroth, A., and Nilsson, M. B.: A 12 year record reveals pre-growing season temperature and water table level threshold effects on the net carbon dioxide exchange in a boreal fen, *Environ. Res. Lett.*, 9, 055006, 2014.

Porada, P., Weber, B., Elbert, W., Pöschl, U., and Kleidon, A.: Estimating global carbon uptake by lichens and bryophytes with a process-based model, *Biogeosciences*, 10, 6989–6989, 2013,

<http://www.biogeosciences.net/10/6989/2013/>.

Price, J. S. and Whittington, P. N.: Water flow in Sphagnum hummocks: mesocosm measurements and modelling, *J. Hydrol.*, 381, 333–340, 2010.

Price, J. S., Whittington, P. N., Elrick, D. E., Strack, M., Brunet, N., and Faux, E.: A method to determine unsaturated hydraulic conductivity in living and undecomposed moss, *Soil Sci. Soc. Am. J.*, 72, 487–491, 2008.

Reich, P. B., Ellsworth, D. S., and Walters, M. B.: Leaf structure (specific leaf area) modulates photosynthesis–nitrogen relations: evidence from within and across species and functional groups, *Funct. Ecol.*, 12, 948–958, 1998.

Rice, S. K., Aclander, L., and Hanson, D. T.: Do bryophyte shoot systems function like vascular plant leaves or canopies? Functional trait relationships in Sphagnum mosses (Sphagnaceae), *Am. J. Bot.*, 95, 1366–1374, 2008.

Robroek, B. J. M., Schouten, M. G. C., Limpens, J., Berendse, F., and Poorter, H.: Interactive effects of water table and precipitation on net CO₂ assimilation of three co-occurring Sphag-

Integrating peatlands into the coupled Canadian Land Surface Scheme

Y. Wu et al.

Title Page

Abstract

Introduction

Conclusions

References

Tables

Figures

⏪

⏩

◀

▶

Back

Close

Full Screen / Esc

Printer-friendly Version

Interactive Discussion

num mosses differing in distribution above the water table, *Glob. Change Biol.*, 15, 680–691, 2009.

Roulet, N. T., Lafleur, P. M., Richard P. J., Moore T. R., Humphreys E. R., and Bubier J.: Contemporary carbon balance and late Holocene carbon accumulation in a northern peatland, *Glob. Change Biol.*, 13, 397–411, 2007.

R Core Team: R: A language and environment for statistical computing, R Foundation for Statistical Computing, Vienna, Austria, available at: <http://www.R-project.org/>, 2014.

Sagerfors, J., Lindroth, A., Grelle, A., Klemetsson, L., Weslien, P., and Nilsson, M.: Annual CO₂ exchange between a nutrient-poor, minerotrophic, boreal mire and the atmosphere, *J. Geophys. Res.-Biogeo.*, 113, G01001, doi:10.1029/2006JG000306, 2008.

Schneider von Deimling, T., Meinshausen, M., Levermann, A., Huber, V., Frieler, K., Lawrence, D. M., and Brovkin, V.: Estimating the near-surface permafrost-carbon feedback on global warming, *Biogeosciences*, 9, 649–665, doi:10.5194/bg-9-649-2012, 2012.

Schuldt, R., Brovkin, V., Kleinen, T., and Winderlich, J.: Modelling holocene carbon accumulation and methane emissions of boreal wetlands: an earth system model approach, *Biogeosciences*, 10, 1659–1674, 2013, <http://www.biogeosciences.net/10/1659/2013/>.

Seneviratne, S. I., Corti, T., Davin, E. L., Hirschi, M., Jaeger, E. B., Lehner, I., Orlowsky, B., and Teuling, A. J.: Investigating soil moisture–climate interactions in a changing climate: a review, *Earth-Sci. Rev.*, 99, 125–161, 2010.

Spahni, R., Joos, F., Stocker, B. D., Steinacher, M., and Yu, Z. C.: Transient simulations of the carbon and nitrogen dynamics in northern peatlands: from the Last glacial maximum to the 21st century, *Clim. Past*, 9, 1287–1308, 2013, <http://www.clim-past.net/9/1287/2013/>.

St-Hilaire, F., Wu, J., Roulet, N. T., Frolking, S., Lafleur, P. M., Humphreys, E. R., and Arora, V.: McGill wetland model: evaluation of a peatland carbon simulator developed for global assessments, *Biogeosciences*, 7, 3517–3530, doi:10.5194/bg-7-3517-2010, 2010.

Suni, T., Berninger, F., Vesala, T., Markkanen, T., Hari, P., Mäkelä, A., Ilvesniemi, H., Nikinmaa E., Hänninen H., Laurila T., Aurela M., Grelle A., Lindroth A., Arneth A., Lloyd J., and Shibistova O.: Air temperature triggers the recovery of evergreen boreal forest photosynthesis in spring, *Glob. Change Biol.*, 9, 1410–1426, 2003.

Integrating peatlands into the coupled Canadian Land Surface Scheme

Y. Wu et al.

[Title Page](#)

[Abstract](#)

[Introduction](#)

[Conclusions](#)

[References](#)

[Tables](#)

[Figures](#)

[⏪](#)

[⏩](#)

[◀](#)

[▶](#)

[Back](#)

[Close](#)

[Full Screen / Esc](#)

[Printer-friendly Version](#)

[Interactive Discussion](#)



Syed, K. H., Flanagan, L. B., Carlson, P. J., Glenn, A. J., and Van Gaalen, K. E.: Environmental control of net ecosystem CO₂ exchange in a treed, moderately rich fen in northern Alberta, *Agr. Forest Meteorol.*, 140, 97–114, 2006.

Talbot, J., Richard, P. J. H., Roulet, N. T., and Booth, R. K.: Assessing long-term hydrological and ecological responses to drainage in a raised bog using paleoecology and a hydrosequence, *J. Veg. Sci.*, 21, 143–156, 2010.

Tarnocai, C.: The effect of climate change on carbon in Canadian peatlands, *Global Planet Change*, 53, 222–232, 2006.

Todd-Brown, K. E. O., Randerson, J. T., Post, W. M., Hoffman, F. M., Tarnocai, C., Schuur, E. A. G., and Allison, S. D.: Causes of variation in soil carbon simulations from CMIP5 Earth system models and comparison with observations, *Biogeosciences*, 10, 1717–1736, doi:10.5194/bg-10-1717-2013, 2013.

Todd-Brown, K. E. O., Randerson, J. T., Hopkins, F., Arora, V., Hajima, T., Jones, C., Shevliakova, E., Tjiputra, J., Volodin, E., Wu, T., Zhang, Q., and Allison, S. D.: Changes in soil organic carbon storage predicted by Earth system models during the 21st century, *Biogeosciences*, 11, 2341–2356, doi:10.5194/bg-11-2341-2014, 2014.

Turetsky, M. R.: The role of bryophytes in carbon and nitrogen cycling, *Bryologist*, 106, 395–409, 2003.

Turetsky, M. R., Bond-Lamberty, B., Euskirchen, E., Talbot, J., Frolking, S., McGuire, A. D., and Tuittila, E.-S.: The resilience and functional role of moss in boreal and arctic ecosystems, *New Phytol.*, 196, 49–67, doi:10.1111/j.1469-8137.2012.04254.x, 2012.

Verseghy, D. L.: CLASS – a Canadian land surface scheme for GCMs, I. Soil model, *Int. J. Climatol.*, 11, 111–133, 1991.

Verseghy, D. L.: CLASS – the Canadian Land Surface Scheme (Version 3.6), Technical Documentation, Tech. rep., Science and Technology Branch, Environment Canada, Toronto, 2012.

Verseghy, D. L., McFarlane, N. A., and Lazare, M.: CLASS – a Canadian land surface scheme for GCMs, II. Vegetation model and coupled runs, *Int. J. Climatol.*, 13, 347–370, 1993.

Vitt, D. H.: A key and review of bryophytes common in North American peatlands, *Evansia*, 31, 121–158, 2014.

Wang, H., Richardson, C. J., and Ho, M.: Dual controls on carbon loss during drought in peatlands, *Nature Climate Change*, 5, 584–587, 2015.

Integrating peatlands into the coupled Canadian Land Surface Scheme

Y. Wu et al.

Title Page

Abstract

Introduction

Conclusions

References

Tables

Figures



Back

Close

Full Screen / Esc

Printer-friendly Version

Interactive Discussion



Wania, R., Ross, I., and Prentice, I. C.: Integrating peatlands and permafrost into a dynamic global vegetation model: 1. Evaluation and sensitivity of physical land surface processes, *Global Biogeochem. Cy.*, 23, GB3014, doi:10.1029/2008GB003412, 2009a.

Wania, R., Ross, I., and Prentice, I. C.: Integrating peatlands and permafrost into a dynamic global vegetation model: 2. Evaluation and sensitivity of vegetation and carbon cycle processes, *Global Biogeochem. Cy.*, 23, GB3015, doi:10.1029/2008GB003413, 2009b.

Ward, S. E., Ostle, N. J., Oakley, S., Quirk, H., Henrys, P. A., and Bardgett, R. D.: Warming effects on greenhouse gas fluxes in peatlands are modulated by vegetation composition, *Ecol. Lett.*, 16, 1285–1293, 2013.

Wu, Y. and Blodau, C.: PEATBOG: a biogeochemical model for analyzing coupled carbon and nitrogen dynamics in northern peatlands, *Geosci. Model Dev.*, 6, 1173–1207, 2013.

Wu, J. and Roulet, N. T.: Climate change reduces the capacity of northern peatlands to absorb the atmospheric carbon dioxide: the different responses of bogs and fens, *Global Biogeochem. Cy.*, 28, 1005–1024, 2014.

Wu, J., Roulet, N. T., Sagerfors, J., and Nilsson, M. B.: Simulation of six years of carbon fluxes for a sedge-dominated oligotrophic minerogenic peatland in Northern Sweden using the McGill Wetland Model (MWM), *J. Geophys. Res., Biogeosciences*, 118, 795–807, 2013, <http://www.biogeosciences.net/118/795/2013/>.

Yebra, M., Van Dijk, A. I., Leuning, R., and Guerschman, J. P.: Global vegetation gross primary production estimation using satellite-derived light-use efficiency and canopy conductance, *Remote Sens. Environ.*, 163, 206–216, 2015.

Yu, Z.: Holocene carbon flux histories of the world's peatlands global carbon-cycle implications, *The Holocene*, 21, 761–774, 2011.

Yu, Z., Loisel, J., Brosseau, D. P., Beilman, D. W., and Hunt, S. J.: Global peatland dynamics since the Last Glacial Maximum, *Geophys. Res. Lett.*, 37, L13402, doi:10.1029/2010GL043584, 2010.

Yu, Z., Loisel, J., Turetsky, M. R., Cai, S., Zhao, Y., Froking, S., MacDonald, G. M., and Bubier, J. L.: Evidence for elevated emissions from high-latitude wetlands contributing to high atmospheric CH₄ concentration in the early Holocene, *Global Biogeochem. Cy.*, 27, 131–140, 2013.

Yurova, A., Wolf, A., Sagerfors, J., and Nilsson, M.: Variations in net ecosystem exchange of carbon dioxide in a boreal mire: modeling mechanisms linked to water table position, *J. Geophys. Res.-Biogeoe.*, 112, doi:10.1029/2006JG000342, 2007.

Integrating peatlands into the coupled Canadian Land Surface Scheme

Y. Wu et al.

Title Page

Abstract

Introduction

Conclusions

References

Tables

Figures

◀

▶

◀

▶

Back

Close

Full Screen / Esc

Printer-friendly Version

Interactive Discussion



Table 2. Descriptions of vegetation characteristics for the four peatland PFTs. A dash (–) indicates the parameter is inapplicable to that PFT.

Parameter name	Description	Unit	Moss	Evergreen shrubs	Deciduous shrubs	Sedge	References
abar	Parameter determines root distribution	–	–	8.50	9.50	9.50	¹
avertmas	Average root biomass for estimating rooting profile	kg Cm ⁻²	–	1.50	1.20	0.20	¹
bsratelt	Litter respiration rate at 15 °C	kg C kg C ⁻¹ yr ⁻¹	–	0.4453	0.5986	0.5260	²
bsratesc	Soil C respiration rates at 15 °C	kg C kg C ⁻¹ yr ⁻¹	–	0.0208	0.0208	0.0100	²
bsrtroot	Base respiration rates at 15 °C for root	kg C kg C ⁻¹ yr ⁻¹	–	0.5000	0.2850	0.1000	²
bsrtstem	Base respiration rates at 15 °C for stem	kg C kg C ⁻¹ yr ⁻¹	–	0.0700	0.0335	–	²
cdlsrtmx	Maximum loss rate for cold stress	day ⁻¹	–	0.10	0.30	0.15	²
drlsrtmx	Maximum loss rate for drought stress	day ⁻¹	–	0.006	0.005	0.020	²
humifac	Humification factor used for transferring C from litter into soil C pool	–	–	0.42	0.42	0.42	²
kn	Canopy light/nitrogen extinction coefficient	–	–	0.50	0.50	0.46	²
laimax	Maximum leaf area index	m ²	–	4.0	3.0	4.0	²
laimin	Minimum leaf area index	m ²	–	1.0	1.0	0.01	²
lfespany	Leaf life span	year	–	5.0	0.4	1.0	³
lwrtshrsh	Lower temperature threshold for cold stress related leaf loss rate	°C	–	–50.0	–5.0	0.1	²
mxrtdpth	Maximum rooting depth	m	–	1.00	1.00	1.00	¹
rmlcoeff	Leaf maintenance respiration coefficient	–	–	0.025	0.020	0.015	²
rmlmoss25	Base dark respiration rate in mosses	μmol CO ₂ m ⁻² s ⁻¹	1.1	–	–	–	⁴
rootlife	Turnover time scale for root	year	–	11.50	12.00	2.00	^{2,5}
rtsrmin	Minimum root/shoot ratio	–	–	0.16	0.16	0.30	^{2,6}
stemlife	Turnover time scale for stem	year	–	65	75	–	²
Tlow	Lower temperature limits for photosynthesis	°C	0.5	–2.0	–2.0	–1.0	^{2,7,8}
Tup	Upper temperature limits for photosynthesis	°C	–	34.0	34.0	40.0	²
V _{max}	Maximum photosynthesis rate	μmol CO ₂ m ⁻² s ⁻¹	6.5, 14 ¹⁰	60	50	40	^{4,9}

¹ calibrated based on proper rooting depth;

² adapted from the parameters for evergreen, deciduous needleleaf and C3 grasses;

³ Lamberty et al. (2007);

⁴ Williams and Flanagan (1998);

⁵ modified for shrubs so that the root turnover time follows trees > shrubs > grasses;

⁶ calibrated based on Murphy et al. (2009) for the minimum root/shoot ratio of sedge to be lower than grasses;

⁷ Moore et al. (2006);

⁸ Tanja et al. (2003);

⁹ Assumed based on literature (Givinish, 2002; Reich, 1998) so that V_{max} values are higher in evergreens than in deciduous and are in line with the values for trees;

¹⁰ V_{max} of mosses is 14 in the summer and 6.5 in the remaining time (Williams and Flanagan, 1998).

Integrating peatlands into the coupled Canadian Land Surface Scheme

Y. Wu et al.

Title Page

Abstract

Introduction

Conclusions

References

Tables

Figures



Back

Close

Full Screen / Esc

Printer-friendly Version

Interactive Discussion



Table 3. Soil decomposition parameters for bog and fen (reformulated from the McGill Wetland Model).

	k_1 ($\mu\text{molCkgC}^{-1}\text{s}^{-1}$)	k_2 (m^{-1})	k_3 ($\mu\text{molCkgC}^{-1}\text{s}^{-1}$)	k_4 ($\mu\text{molCkgC}^{-1}\text{s}^{-1}$)	k_5 (m^{-1})	k_6 (m^{-1})	k_7 ($\mu\text{molCkgC}^{-1}\text{s}^{-1}$)	k_8 ($\mu\text{molCkgC}^{-1}\text{s}^{-1}$)	k_9 (m^{-2})	k_{10} (m^{-1})
Bog	0.009	-20.0	0.015	-0.183	-18.0	0.003	0.0134	0.0044		
Fen	0.010	-40.0	0.015	-1.120	-25.0	0.000	0.0151	-0.0052	4.057	72.067

Integrating peatlands into the coupled Canadian Land Surface Scheme

Y. Wu et al.

Table 5. Summary of statistics of model performance with respect to latent heat flux (QH), sensible heat flux (QE) and soil T at 5 cm (T_{s5}). * indicates unrealistic values observed for the site.

Site		Bog			Fen				Mean	
		MB-Bog	SE-Faj	RU-Fyo	UK-Amo	AB-Fen	FI-Kaa	FI-Lom		SE-Deg
QH (Wm^{-2})	r^2	0.65	0.50	0.41	0.22	0.89	0.25	0.42	0.39	0.47
	RMSE	23.0	27.3	37.7	31.0	41.5	36.7	25.4	19.6	30.3
QE (Wm^{-2})	r^2	0.89	0.56	0.51	0.01*	0.82	0.35	0.49	0.54	0.52
	RMSE	27.3	33.5	33.3	79.7	15.8	31.5	28.3	23.9	34.1
T_{s5} ($^{\circ}\text{C}$)	r^2	0.98	0.87	0.88	0.77	0.91	0.85	0.90	0.79	0.87
	RMSE	1.7	2.6	4.6	2.3	4.7	2.9	2.1	3.86	3.1

Title Page

Abstract

Introduction

Conclusions

References

Tables

Figures

⏪

⏩

◀

▶

Back

Close

Full Screen / Esc

Printer-friendly Version

Interactive Discussion



Integrating peatlands into the coupled Canadian Land Surface Scheme

Y. Wu et al.

Table 6. Summary of statistics of model performance with respect to GPP, ER and NEP ($\text{g C m}^{-2} \text{ day}^{-1}$).

Site		Bog			Fen				Mean	
		MB-Bog	SE-Faj	RU-Fyo	UK-Amo	AB-Fen	FI-Kaa	FI-Lom		SE-Deg
Daily GPP	r^2	0.95	0.79	0.81	0.63	0.95	0.78	0.76	0.65	0.79
($\text{g C m}^{-2} \text{ d}^{-1}$)	RMSE	0.648	0.606	2.361	1.440	1.454	0.601	1.066	0.839	1.13
Daily ER	r^2	0.96	0.75	0.62	0.55	0.93	0.61	0.84	0.54	0.73
($\text{g C m}^{-2} \text{ d}^{-1}$)	RMSE	0.562	0.567	2.849	1.122	0.867	0.546	0.497	0.615	0.95
Daily NEP	r^2	0.67	0.17	0.31	0.16	0.72	0.35	0.36	0.41	0.39
($\text{g C m}^{-2} \text{ d}^{-1}$)	RMSE	1.571	0.578	1.633	0.926	1.014	0.589	0.993	0.486	0.97

Title Page

Abstract

Introduction

Conclusions

References

Tables

Figures

⏪

⏩

◀

▶

Back

Close

Full Screen / Esc

Printer-friendly Version

Interactive Discussion



Integrating peatlands into the coupled Canadian Land Surface Scheme

Y. Wu et al.

Table 7. Summary of observed (obs.) and modeled (mod.) mean annual GPP, ER and NEP of the 8 sites with standard deviation shown in brackets; units are $\text{g C m}^{-2} \text{yr}^{-1}$.

Site	Bog			Fen				Mean	
	MB-Bog	SE-Faj	RU-Fyo	UK-Amo	AB-Fen	FI-Kaa	FI-Lom		SE-Deg
GPP obs.	714(±45)	472(±3)	1502(±251)	789(±189)	864 (±172)	289 (±39)	418(±52)	383(±24)	679
GPP mod.	734(±15)	573(±49)	1135(±4)	752(±37)	594 (±72)	327 (±33)	489(±39)	300(±71)	613
ER obs.	612(±29)	536(±102)	1545(±119)	706(±212)	678 (±160)	270 (±40)	380(±59)	295(±36)	628
ER mod.	690(±89)	426(±55)	1000(±86)	594(±46)	581 (±88)	270 (±46)	372(±96)	224(±76)	520
NEP obs.	103(±25)	25(±34)	-17(±73)	87(±48)	187 (±37)	17 (±29)	57(±9)	58(±6)	65
NEP mod.	44(±78)	97(±77)	135(±91)	157(±43)	13 (63)	57 (±22)	117(±57)	77(±5)	87

Title Page

Abstract

Introduction

Conclusions

References

Tables

Figures



Back

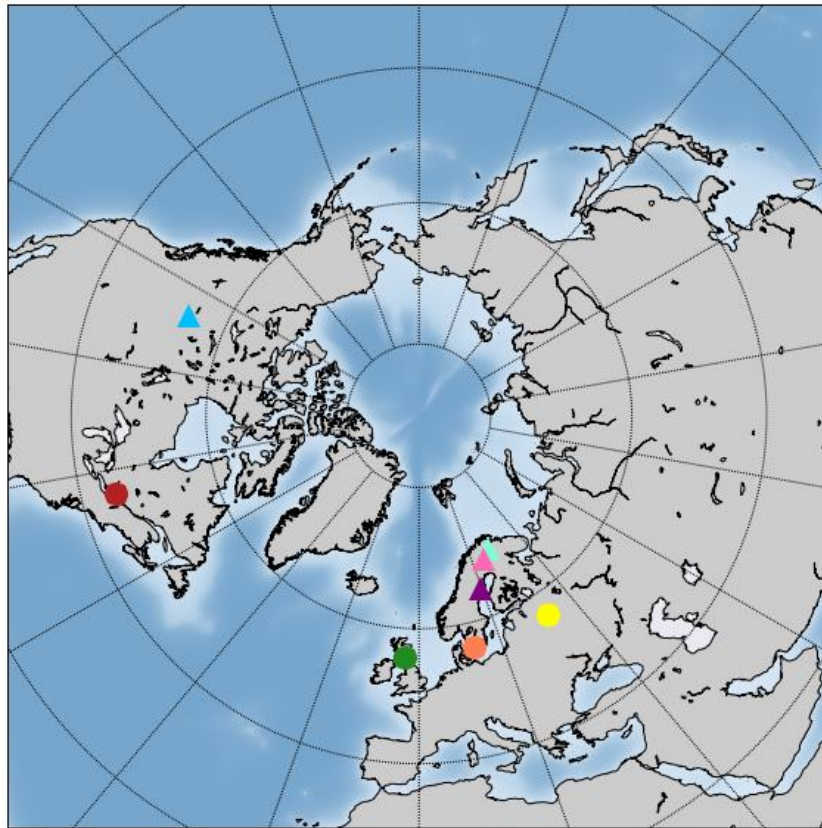
Close

Full Screen / Esc

Printer-friendly Version

Interactive Discussion





- MB-Bog
- SE-Faj
- RU-Fyo
- UK-Amo
- ▲ AB-Fen
- ▲ FI-Kaa
- ▲ FI-Lom
- ▲ SE-Deg

Figure 2. Locations of the test peatlands; closed circles indicate bogs and triangles indicate fens.

Integrating peatlands into the coupled Canadian Land Surface Scheme

Y. Wu et al.

Title Page	
Abstract	Introduction
Conclusions	References
Tables	Figures
⏪	⏩
◀	▶
Back	Close
Full Screen / Esc	
Printer-friendly Version	
Interactive Discussion	



Integrating peatlands into the coupled Canadian Land Surface Scheme

Y. Wu et al.

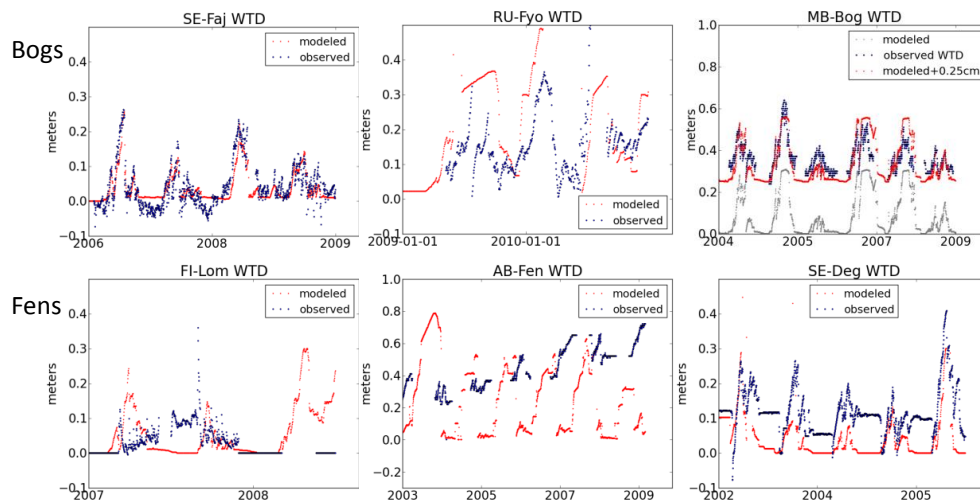


Figure 3. Simulated and observed daily average water table depth (m) in three bogs (MB-Bog, RU-Fyo, SE-Faj) and three fens (AB-Fen, FI-Lom, SE-Deg).

Title Page

Abstract

Introduction

Conclusions

References

Tables

Figures



Back

Close

Full Screen / Esc

Printer-friendly Version

Interactive Discussion



Integrating peatlands into the coupled Canadian Land Surface Scheme

Y. Wu et al.

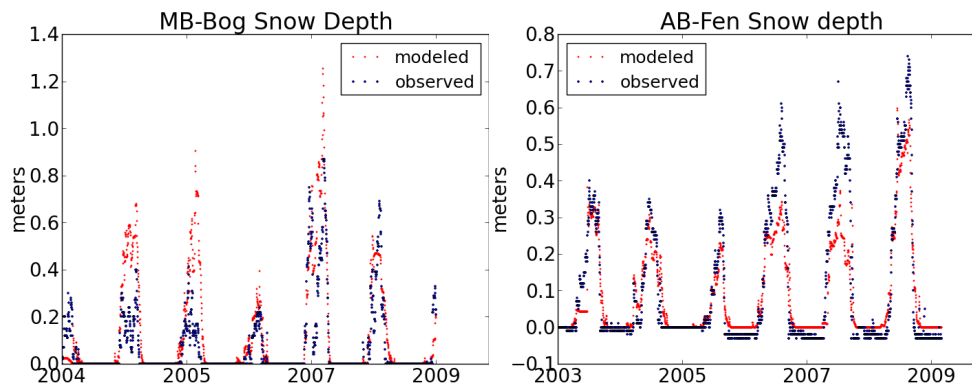


Figure 4. Simulated and observed daily average snow depth (m) in the MB-Bog and the AB-Fen.

[Title Page](#)[Abstract](#)[Introduction](#)[Conclusions](#)[References](#)[Tables](#)[Figures](#)[⏪](#)[⏩](#)[◀](#)[▶](#)[Back](#)[Close](#)[Full Screen / Esc](#)[Printer-friendly Version](#)[Interactive Discussion](#)

Integrating peatlands into the coupled Canadian Land Surface Scheme

Y. Wu et al.

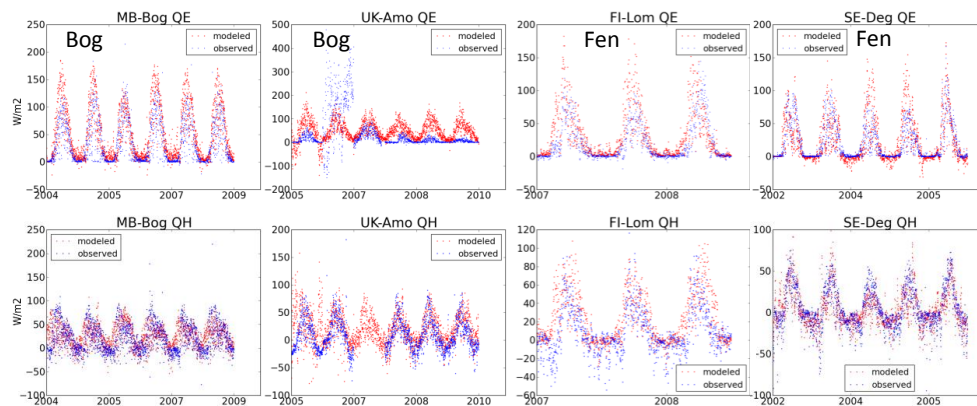


Figure 5. Simulated and observed daily average latent heat flux QE (W m^{-2}) and sensible heat flux QH (W m^{-2}) in two bogs (MB-Bog and UK-Amo) and two fens (FI-Lom and SE-Deg).

Title Page

Abstract

Introduction

Conclusions

References

Tables

Figures

⏪

⏩

◀

▶

Back

Close

Full Screen / Esc

Printer-friendly Version

Interactive Discussion



Integrating peatlands into the coupled Canadian Land Surface Scheme

Y. Wu et al.

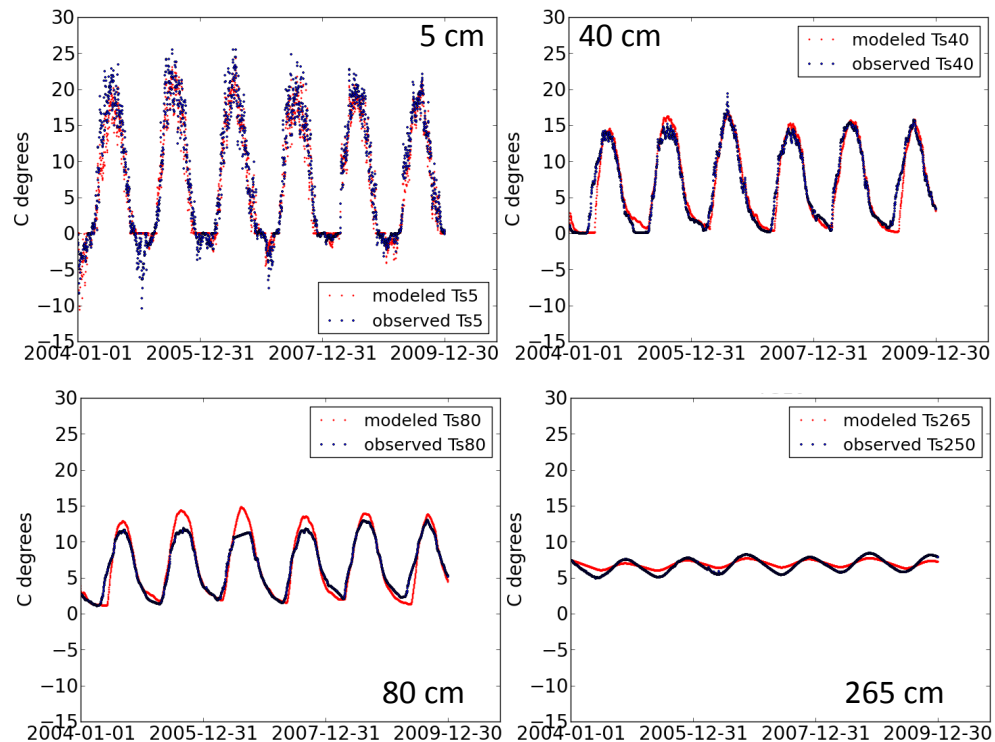


Figure 6. Simulated and observed daily mean soil temperature T_s ($^{\circ}\text{C}$) at 5, 40, 80 and 250 cm at the Mer Bleue Bog. Note that the simulated temperatures at 40 and 80 cm are interpolated from the simulated soil layer temperatures above and below these depths.

Title Page

Abstract

Introduction

Conclusions

References

Tables

Figures

◀

▶

◀

▶

Back

Close

Full Screen / Esc

Printer-friendly Version

Interactive Discussion



Integrating peatlands
into the coupled
Canadian Land
Surface Scheme

Y. Wu et al.

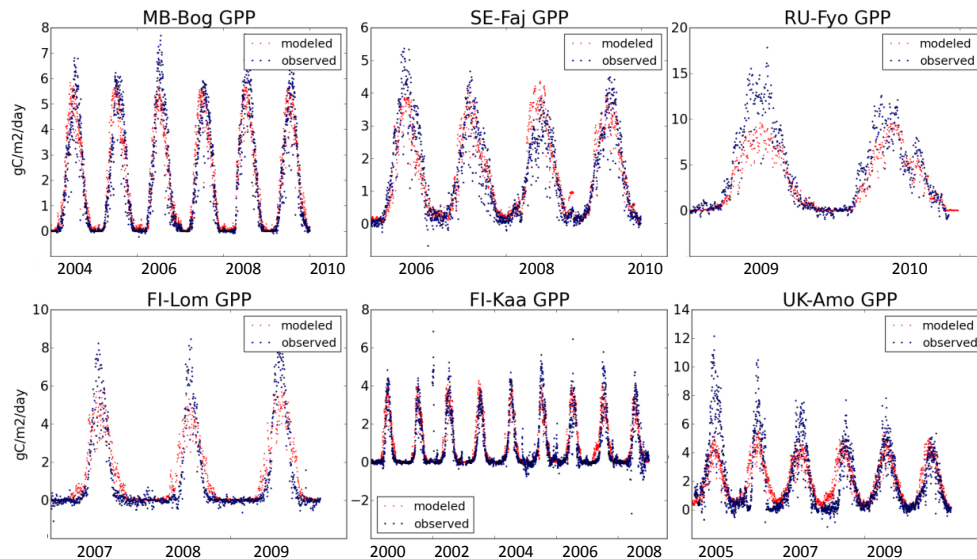


Figure 7. Simulated and observed daily GPP (gC m⁻² day⁻¹) in bogs and fens.

[Title Page](#)[Abstract](#)[Introduction](#)[Conclusions](#)[References](#)[Tables](#)[Figures](#)[⏪](#)[⏩](#)[◀](#)[▶](#)[Back](#)[Close](#)[Full Screen / Esc](#)[Printer-friendly Version](#)[Interactive Discussion](#)

Integrating peatlands into the coupled Canadian Land Surface Scheme

Y. Wu et al.

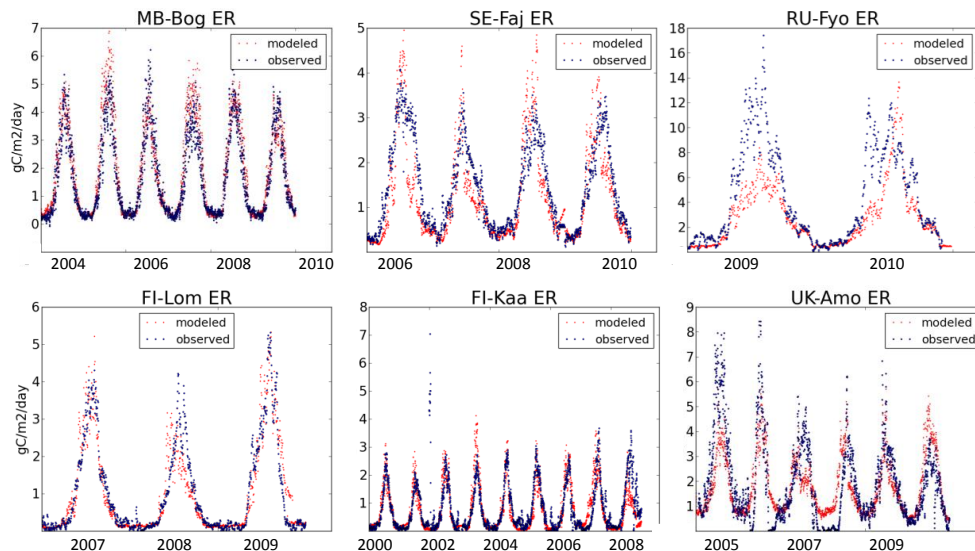


Figure 8. Simulated and observed daily ER ($\text{gC m}^{-2} \text{day}^{-1}$) in bogs and fens.

Title Page

Abstract

Introduction

Conclusions

References

Tables

Figures

⏪

⏩

◀

▶

Back

Close

Full Screen / Esc

Printer-friendly Version

Interactive Discussion



Integrating peatlands into the coupled Canadian Land Surface Scheme

Y. Wu et al.

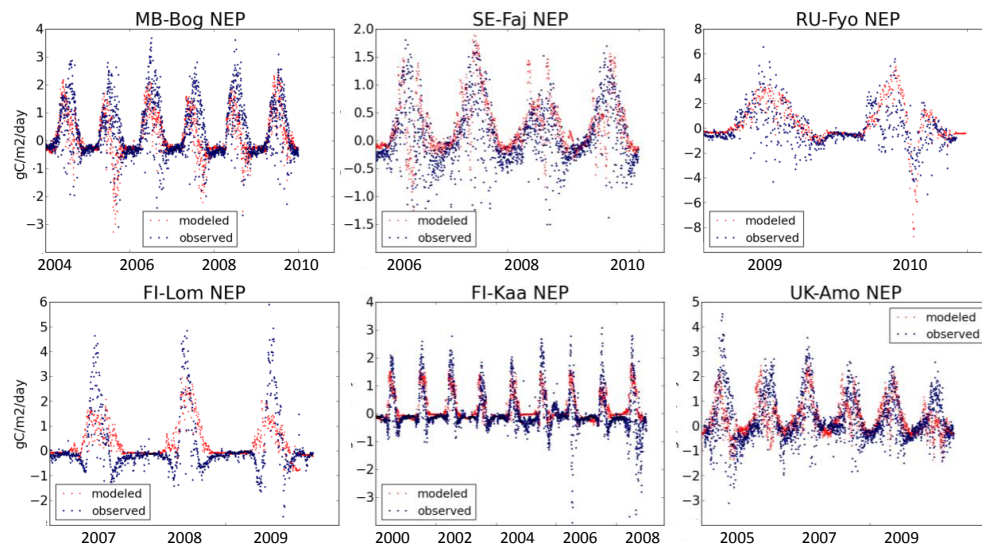


Figure 9. Simulated and observed daily NEP ($\text{gC m}^{-2} \text{day}^{-1}$) in bogs and fens.

Title Page

Abstract

Introduction

Conclusions

References

Tables

Figures

⏪

⏩

◀

▶

Back

Close

Full Screen / Esc

Printer-friendly Version

Interactive Discussion



Integrating peatlands into the coupled Canadian Land Surface Scheme

Y. Wu et al.

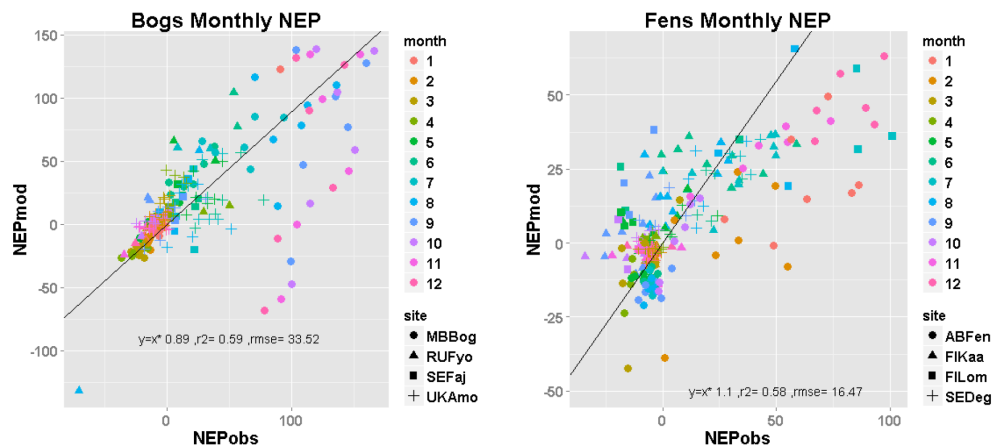


Figure 10. Scatter plots of simulated and observed monthly mean NEP ($\text{gCm}^{-2} \text{month}^{-1}$) in bogs and fens. The sites are represented by different symbols and NEP for each of the 12 months is colour-coded. The black line represents the best fit of the modelled NEP and the observed NEP.

Title Page

Abstract

Introduction

Conclusions

References

Tables

Figures

⏪

⏩

◀

▶

Back

Close

Full Screen / Esc

Printer-friendly Version

Interactive Discussion



Integrating peatlands into the coupled Canadian Land Surface Scheme

Y. Wu et al.

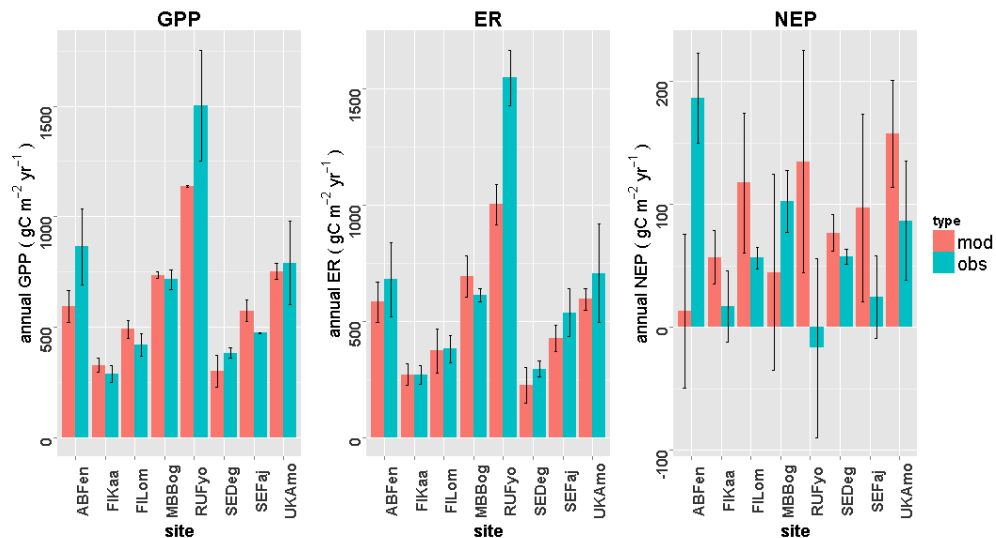


Figure 11. Observed and simulated annual GPP, ER and NEP ($\text{gC m}^{-2} \text{yr}^{-1}$) for the eight sites (error bars show the standard deviations), red bars are modeled fluxes and blue bars are observed fluxes.

Title Page

Abstract Introduction

Conclusions References

Tables Figures

◀ ▶

◀ ▶

Back Close

Full Screen / Esc

Printer-friendly Version

Interactive Discussion

Integrating peatlands into the coupled Canadian Land Surface Scheme

Y. Wu et al.

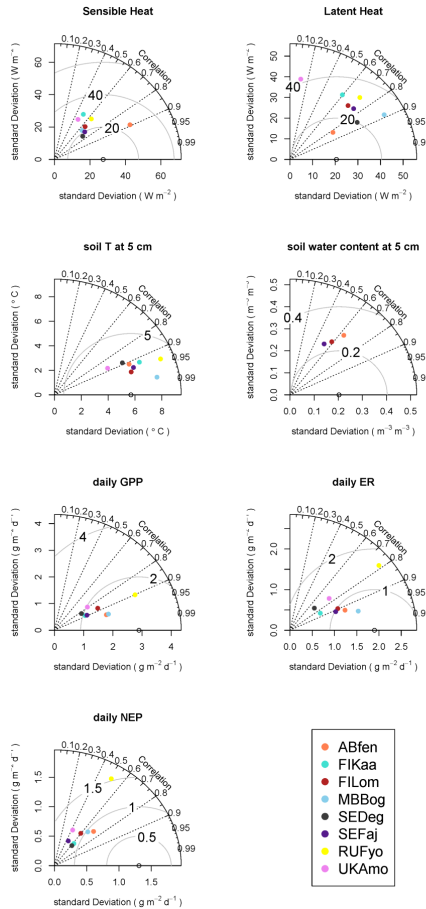


Figure 12. Taylor diagram of model performance on sensible heat (QH), latent heat (QE), soil temperature and water content at 5 cm depth, daily GPP, ER and NEP ($\text{g C m}^{-2} \text{ day}^{-1}$) in bogs and fens.

Title Page

Abstract

Introduction

Conclusions

References

Tables

Figures

⏪

⏩

◀

▶

Back

Close

Full Screen / Esc

Printer-friendly Version

Interactive Discussion



Integrating peatlands into the coupled Canadian Land Surface Scheme

Y. Wu et al.

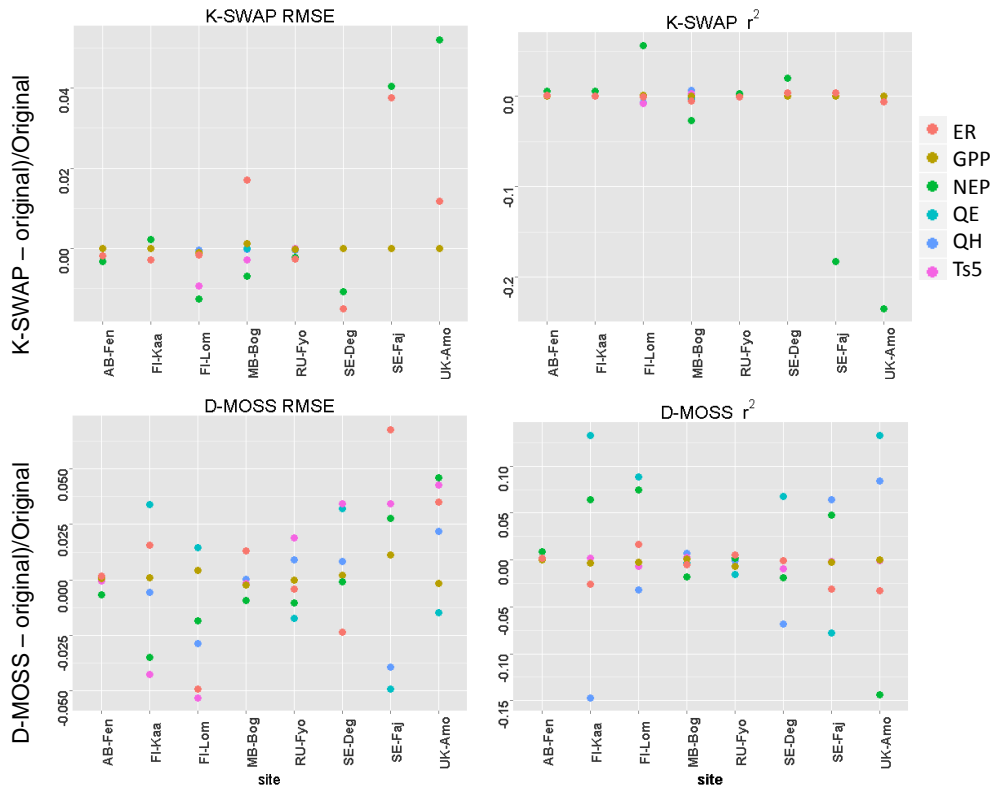


Figure 13. Comparisons of RMSE and r^2 of the simulated latent heat flux (QE), sensible heat flux (QH), soil temperature at 5 cm depth (T_{s5}), GPP, ER and NEP against the original simulations for the two tests described in Sect. 4.5.

[Title Page](#)

[Abstract](#)

[Introduction](#)

[Conclusions](#)

[References](#)

[Tables](#)

[Figures](#)

⏪

⏩

◀

▶

[Back](#)

[Close](#)

[Full Screen / Esc](#)

[Printer-friendly Version](#)

[Interactive Discussion](#)

